ELSEVIER

Journal of Non-Crystalline Solids 232–234 (1998) 581–586

JOURNAL OF NON-CRYSTALLINE SOLIDS

Extended X-ray absorption fine structure measurements of the local environment of Pr^{3+} ions in silica xerogels and zinc borate glasses

F. Rocca [a], G. Dalba [b], R. Grisenti [b], M. Bettinelli [c], F. Monti [c,*], A. Kuzmin [d,a]

[a] *CeFSA, Centro CNR-ITC di Fisica degli Stati Aggregati, Via Sommarive 14, 38050 Povo (Trento), Italy*
[b] *Istituto Nazionale di Fisica della Materia and Dipartimento di Fisica, Università di Trento, 38050 Povo (Trento), Italy*
[c] *Facoltà di Scienze dell'Università di Verona, Istituto Policattedra, Strada Le Grazie, 37134 Verona, Italy*
[d] *Institute of Solid State Physics, 8 Kengaraga str., LV-1063 Riga, Latvia*

Abstract

The local environment around Pr^{3+} ions in a silica xerogel, densified at 950°C, and in $4ZnO \cdot 3B_2O_3$ glasses doped with different Pr concentrations (from 0.5 up to 8 mol%) has been studied by X-ray absorption spectroscopy at the Pr L_3-edge. The radial distribution functions (RDF) in the region of the first coordination shell of praseodymium, i.e. the nearest group of oxygen atoms, were reconstructed using a model-independent approach. Both in the xerogel and in the glasses, the RDFs are broad and asymmetric, with a tail on the long distance side and a coordination number ranging between 6 and 7. The RDF of the xerogel is broader and more symmetric and shows a coordination number slightly lower than in the glasses. The local environment of Pr^{3+} in $4ZnO \cdot 3B_2O_3$ glass does not change as a function of the praseodymium content.

1. Introduction

Glasses activated by rare-earth (RE) ions are of great interest because of their applications in photonics and optoelectronics [1]. Among the different lanthanides, Pr^{3+} is an excellent ion for optical applications, such us up-converters and optical amplifiers, mainly because of its optical spectrum [2].

This paper presents a study of the local coordination of Pr^{3+} in two disordered hosts, with differing networks and differing preparation methods, viz. zinc borate glasses of composition $4ZnO \cdot 3B_2O_3$ obtained by melt quenching and a silica xerogel densified at 950°C for 120 h. Both systems have been recently investigated by spectroscopic techniques [3,4] and have quite different dynamics for the relaxation of the electronic states of Pr^{3+}. In particular, the energy transfer by cross-relaxation is very efficient in the xerogels even at the smallest Pr^{3+} content [4].

X-ray absorption spectroscopy (XAS) is a very powerful tool in this field because of its atomic selectivity. The recent development of high intensity synchrotron radiation sources now allows these studies to be extended to low concentrations of absorbing element, by using fluorescence detection techniques.

* Corresponding author. Tel.: 39 45 8098910; fax: 39 45 8098929; e-mail: monti@biotech.sci.univr.it.

0022-3093/98/$19.00
PII: S0022-3093(98)00526-2

2. Experimental procedure and data analysis

Glasses of composition $4ZnO \cdot 3B_2O_3$, doped with 0.5, 1, 2, 4 and 8 mol% of Pr^{3+}, were prepared by mixing appropriate quantities of ZnO (Carlo Erba Analyticals RPE), H_3BO_3 (Carlo Erba Analyticals RPE) and Pr_6O_{11} (Janssen Reagent Grade) in a platinum crucible. The samples were melted at 1250°C for 4 h. Each liquid was then cast in a brass mould and annealed at 500°C for 12 h. Silica xerogel doped with 10 000 ppm Pr/Si were prepared via the hydrolysis and condensation of tetramethylorthosilicate (TMOS), methanol and deionized water, in the presence of nitric acid [5]. The Pr^{3+} ions were introduced in the initial stage of the process, by dissolving $Pr(NO_3)_3 \cdot 6H_2O$ (99.99%, Aldrich) in a methanol/water mixture. The molar ratio in the starting solution was $H_2O:CH_3OH:HNO_3:TMOS = 10:6:0.7:1$. After preparation, the xerogel was densified at 950°C for 120 h.

The reference material used in the EXAFS (Extended X-ray absorption fine structures) analysis was crystalline $PrVO_4$ [6], prepared by a solid-state reaction starting from Pr_6O_{11} and V_2O_5 powders. The powders were ground and mechanically mixed in the appropriate quantities. They were subsequently heated in air at 680°C for 12 h, finely ground and, finally, heated again for 12 h at 1000°C; X-ray diffraction (XRD) measurements confirmed the quality of the final polycrystalline product.

The Pr L_3-edge X-ray absorption spectra were recorded at the European Synchrotron Radiation Facility (ESRF – Grenoble, France) storage ring at the GILDA BM8 beamline. The electron energy was 6 GeV and the maximum stored current 140 mA. The X-ray beam was monochromatized and focused onto the sample by a Si(3 1 1) double-crystal monochromator and its primary intensity was monitored by an ion chamber containing argon gas. The silica xerogel and the glasses doped with 0.5, 1, 2 and 4 mol% of praseodymium were measured in fluorescence mode using a Ge solid state detector in the 90° configuration. The 8 mol% Pr doped glass and the reference crystalline compound, $PrVO_4$, were measured in transmission mode under the same experimental conditions

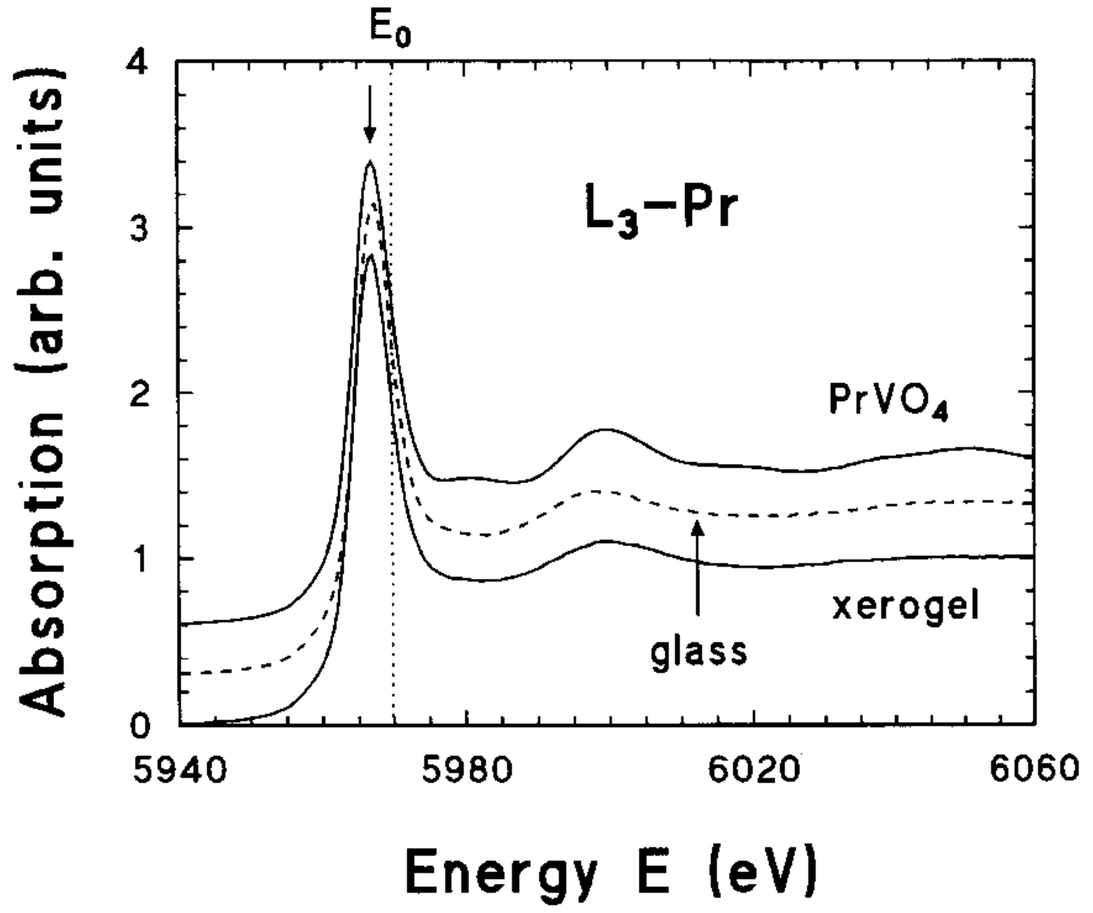

Fig. 1. The XANES region of the Pr L_3-edge spectra for $PrVO_4$, densified silica xerogel and 4 mol% Pr^{3+}-doped zinc borate glass. The white-line (WL) is indicated by an arrow. The position of the photoelectron energy origin, E_0, used in the EXAFS calculations, is shown by the vertical dotted line.

using a second ion chamber to monitor the intensity of X-rays passing through the sample. All of the measurements were performed at room temperature.

The data analysis was performed using the EDA EXAFS data analysis software package [7]. The XANES (X-ray absorption near edge structures) region of the experimental spectra, normalised to the absorption jump, is shown in Fig. 1. The experimental EXAFS signals (Fig. 2(a)) were extracted following a standard procedure [7,8]. The energy origin of the photoelectron $E_0 = 5970$ eV (Fig. 1) was determined by aligning the experimental EXAFS signal with that calculated for the reference compound $PrVO_4$ [9]. The EXAFS calculations for $PrVO_4$ were performed using the FEFF6 code [10] for a cluster centred at the Pr ion and having a radius of approximately 7 Å. The experimental EXAFS signals, $k\chi(k)$, (Fig. 2(a)) were Fourier transformed (FT) in the range 0.5–10.0 $Å^{-1}$ using a Kaiser–Bessel window and back-FT in the 0.5–2.8 Å interval, to single out the contribution of the first coordination shell (Fig. 2(b)). A contribution due to next nearest shells is also resolved, both in the xerogel and in the glasses, and will be briefly discussed later.

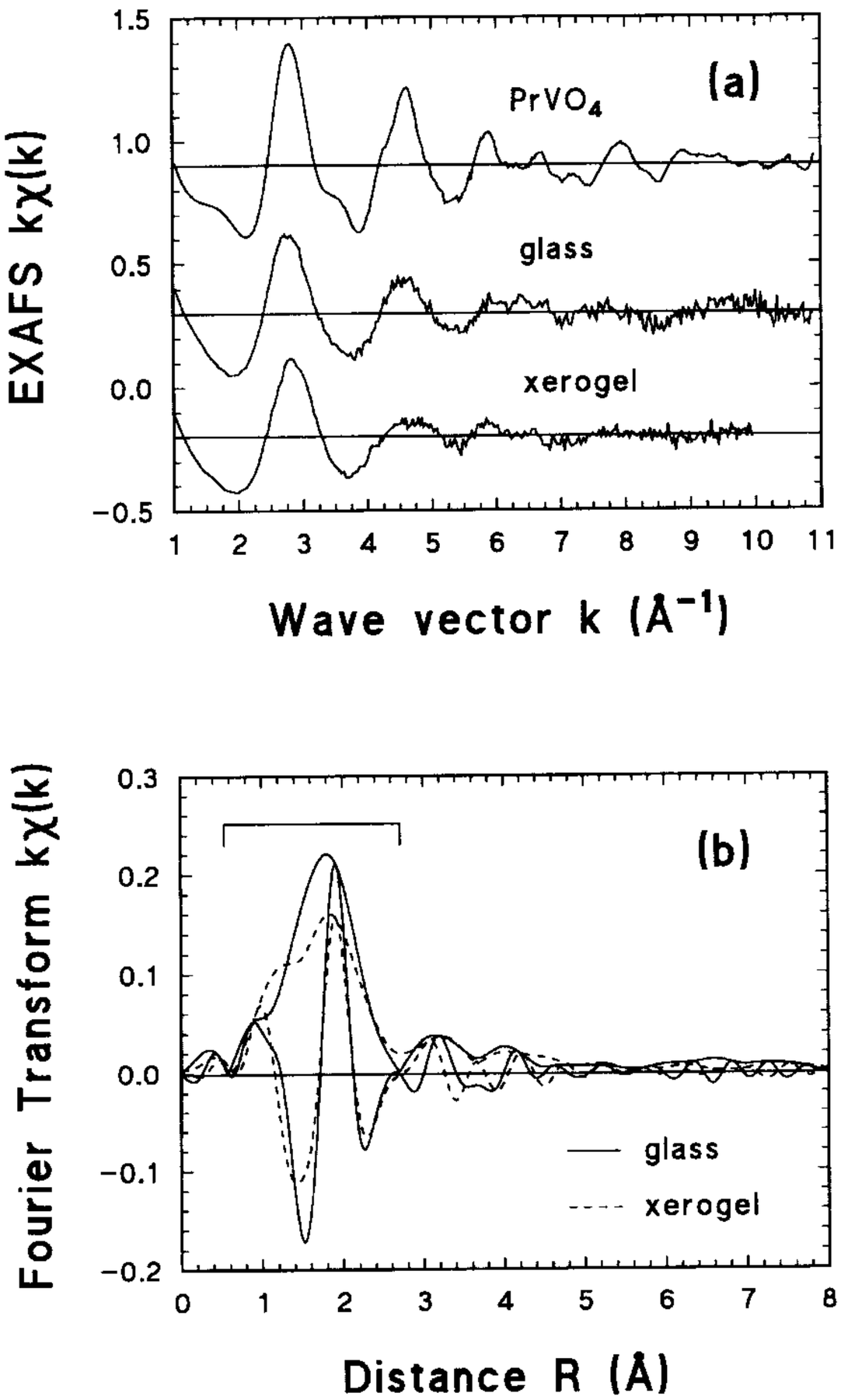

Fig. 2. Experimental Pr L_3-edge EXAFS $k\,\chi(k)$ spectra for the densified silica xerogel (10 000 ppm Pr/Si) and 4 mol% Pr^{3+} doped zinc borate glass (a) and their Fourier transforms (b). The region of the first coordination shell is indicated in (b).

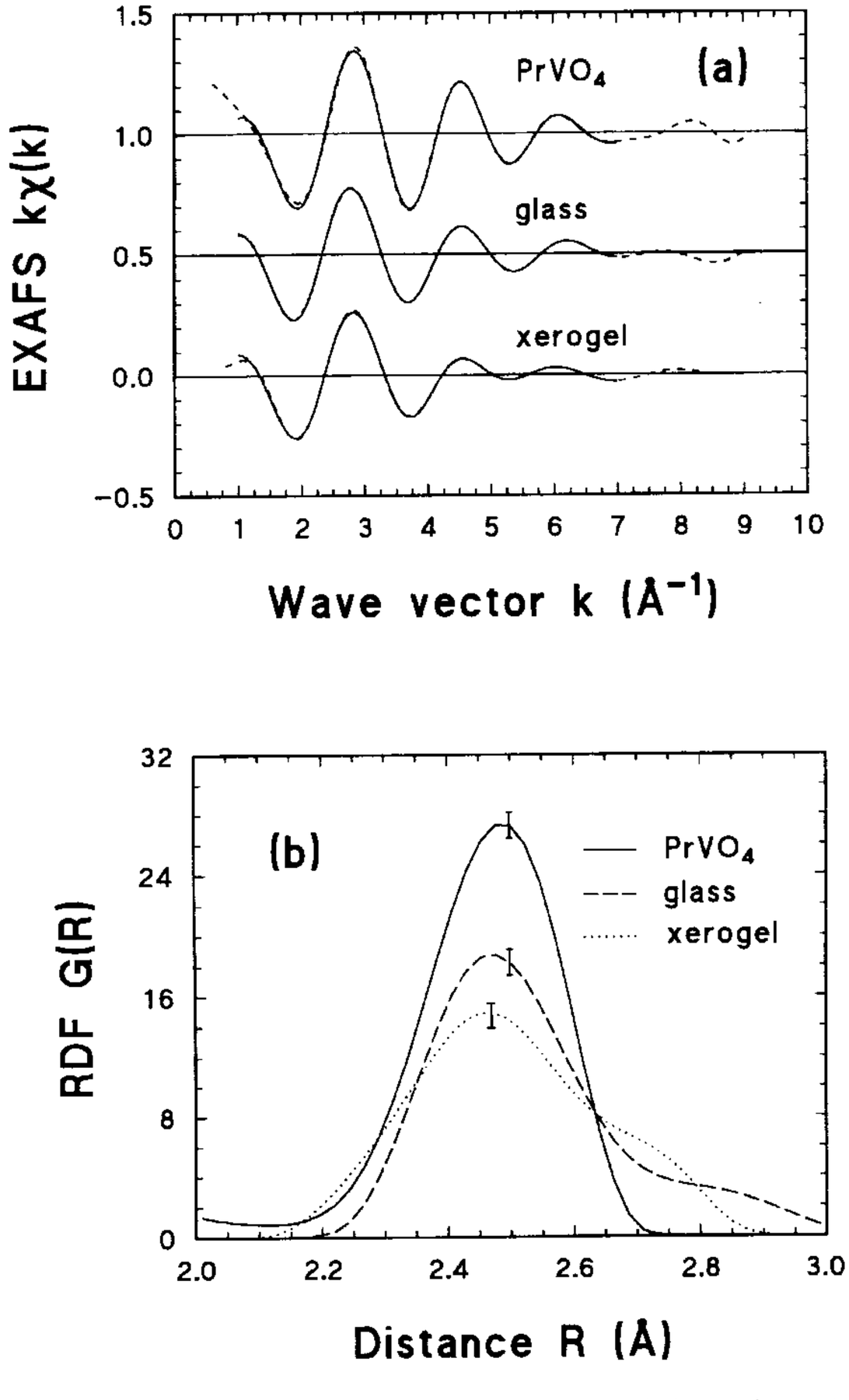

Fig. 3. Results of the fit to the first shell around the Pr ions. (a) the calculated (solid lines) and experimental (dashed lines) EXAFS signals and (b) the resulting RDFs. The error bars indicate the range of uncertainty between different best fit results.

The first shell EXAFS signals obtained, $k\chi(k)$, were fitted (Fig. 3(a)) in the k-space over the range 1–7 Å^{-1}, using the previously determined theoretical backscattering amplitude and phase shift functions for the Pr–O atom pair. The fit was performed in the k-space using the minimization procedure fully described in Refs. [7,8], which allows a model-independent radial distribution function (RDF), G(r), to be reconstructed within the first shell. Details of the method and its application to a set of crystalline and disordered systems can be found in Ref. [8]. The calculated RDFs are presented in Fig. 3(b): the error bars shown in the figure indicate the range of the different values obtained at each r point of the $G(r)$ curves resulting from different parameters in the analysis and best fitting procedure. Since the EXAFS spectra for all of the zinc borate glasses are identical, within the marked experimental error, only the data for the 4 mol% Pr-doped glass are presented in Figs. 2 and 3.

3. Results

The Pr L_3-edge XANES region (Fig. 1) has a strong white line (WL), located just above the

edge, and a fine structure, located above the continuum threshold, E_0. The origin of the WL is the $2p_{3/2} \rightarrow 5\epsilon$,d transition, from the $2p(Pr^{3+})$ core-level into the final relaxed state in the continuum (ϵ) with 5d(Pr)-atomic character [9]. The shape of the WL maximum indicates that praseodymium ions are present only in the Pr^{3+} valence state [11].

The first coordination shell of praseodymium in the xerogel and in the glasses is described by the total RDF shown in Fig. 3(b), which shows the broad asymmetric distribution of the Pr–O distances in these systems. The EXAFS signals corresponding to the RDFs are in good agreement with the experimental ones, as shown in Fig. 3(a). The RDFs obtained can be described by a set of structural parameters (Table 1), such as the total coordination number, N (given by the area under $G(r)$), the position of the maximum, R_{MAX}, the mean Pr–O distance, $\langle R \rangle$, and the variance, σ^2 (mean square relative displacement, MSRD) which represents the sum of the thermal and static disorder. It can be seen (Fig. 3(b) and Table 1) that the position of the maximum in the xerogel and in the glasses is almost the same as in the c-$PrVO_4$ but, at variance with what observed for the reference crystal, the RDFs in the xerogel and glasses are asymmetric with a tail on the longer distance side and a smaller coordination number. Moreover, some differences also exist between the xerogel and the glasses: in the former, the RDF is broader and more symmetric and has a smaller coordination number, as expected from a comparison of the first peak intensities in the Fourier transforms of the EXAFS signals (Fig. 2(b)).

Table 1
Structural parameters for the Pr^{3+} environment obtained from the EXAFS data analysis

Sample	N	R_{MAX} (Å)	$\langle R \rangle$ (Å)	σ^2 (Å^2)
$PrVO_4$	8	2.47	2.47	0.010
Silica xerogel	6.2	2.47	2.50	0.023
Glass 0.5%	7.1	2.47	2.53	0.029
Glass 1%	7.1	2.47	2.53	0.024
Glass 2%	6.5	2.47	2.53	0.020
Glass 4%	6.9	2.47	2.53	0.028
Glass 8%	6.7	2.47	2.53	0.022
Glass (average)	6.9	2.47	2.53	0.025

N (±0.7) is the total coordination number; R_{MAX} (±0.02 Å) is the position of the RDF maximum; $\langle R \rangle$ (±0.02 Å) is the first central moment of the RDF (i.e. the mean Pr–O distance), and σ^2 (±0.005 Å^2) is the second central moment of the RDF (i.e. the variance). The neutron powder diffraction data for $PrVO_4$ are four Oxygen atoms at 2.422 Å and four Oxygen atoms at 2.526 Å, i.e. $N_{tot} = 8$ and $R_{aver} = 2.474$ Å [10].

Similar results, for both the crystal and the glasses, were obtained with different Fourier transform intervals (1.0–7.5 and 1–9 Å^{-1}) and using different k (2.4–7.0 Å^{-1}) and R (1.3–3.3 Å) ranges for the RDF reconstruction: the range of the resulting $G(r)$ functions are clearly indicated by the marked error bars on Fig. 3(b). Moreover, the calculated coordination numbers for the glasses, as well as the mean distances and the MSRD relative to the crystal reference, are in agreement with those determined by the 'ratio-method' using the EXTRA data analysis software package [12].

4. Discussion

A comparison of the EXAFS results obtained for the $4ZnO \cdot 3B_2O_3$ glasses and the densified xerogel is useful, in order to make some comments concerning the differing environments of the Pr^{3+} ions in these systems. The first important point is the constant position of the maximum of the radial distribution (R_{MAX}). This constancy means that the Pr^{3+} ions, in these glasses and in the densified xerogel, have local environments with the preferred Pr–O distance, appropriate to the ionic size [13]. This result is in agreement with spectroscopic measurements on Eu^{3+} silica xerogels [14] and with EXAFS measurements on borosilicate glasses [15]. However, our refined analysis shows that the first coordination shells are distorted, due to the strain imposed by the host systems. The distribution of distances around Pr^{3+} in the xerogel is the most broadened, extending from 2.2 to 3.0 Å. In addition, the RDFs for the xerogel and glasses are asymmetric with a tail at longer distances. The presence of shorter Pr–O bonds in the xerogel is due to the modification of the xerogel matrix during the densification process. In fact, the thermal treatment of xerogels results in a contraction of the whole system due to the progressive dehydration and densification: in course of this process

the Pr^{3+} environment changes from a *wet* state (where its main coordination is similar to that in water solutions) to a *solid* state, which is mainly affected by the contraction of the SiO_2 network. This contraction also results in a decrease of the coordination number, which changes from 8 to 6.2 [9], confirming the results of spectroscopy studies [14].

It should be noted that the local environment of the Pr^{3+} ions is well defined, in spite of the asymmetry and distortion of the first coordination shell, and that the RDF does not change (within our experimental accuracy) on changing the Pr content from 0.5 to 8 mol% in the $4ZnO \cdot 3B_2O_3$ glasses. We can explain this experimental fact in terms of an active role for the Pr^{3+} ions, which locally induce changes in the surrounding structure, without indications of clustering or nucleation. This hypothesis is confirmed by a qualitative analysis of the next nearest neighbour shell. We note a clear difference between the spectra of the xerogel and the glasses, mainly in the imaginary part of the peak centred at 3.2 Å in the Fourier transform (Fig. 2(b)), whereas all of the glasses have similar features in this region.

A quantitative analysis of the next nearest neighbour shell contributions has been performed, but the short range of the experimental data and the quality of the signal allow us only to draw qualitative conclusions. For the xerogel, the EXAFS signal can be modelled by Pr–Si and Pr–Pr contributions: the presence of short Pr–Pr distances agrees with the observed quenching of the luminescence in xerogels [4]. For the glasses, the presence of Pr–Zn and Pr–B contributions is sufficient to yield a satisfactory result: without the contribution from a Pr–Zn distance, the fit becomes worse. The presence in the glasses of a Pr–Pr distance cannot be ruled out at this stage, but the absence of changes as a function of the Pr concentration confirms the absence of clustering. We note that other EXAFS studies (for example of Er^{3+} in different glasses) agree with our conclusion that, for a selected glass system, the local environment does not change as the level of dopant concentration is varied [16].

A final comment can be made concerning the coordination numbers obtained within the first shell: they are reduced with respect to the reference crystal, $PrVO_4$, and there is a difference between the densified xerogel and the glasses: the average number of oxygen neighbours in the xerogel is about 0.6 atoms smaller than in the glasses (Table 1). This decrease can be correlated with the corresponding shift in $\langle R \rangle$, calculated for the asymmetric RDFs: a similar trend has been observed for lanthanide ions in silicate glasses with different amounts of network polymerisation [13]. The possibility of a rearrangement of the network around the rare-earth ions depends on the presence of non-bridging oxygen atoms, and on the RE elements acting as network modifiers. The difference in host systems and preparation conditions can explain the observed difference between the RDFs. The question remains as to the role of the zinc ions, because at this stage we cannot exclude the presence of Pr–O–Zn correlations in the zinc borate glasses.

5. Conclusions

A XANES and EXAFS analysis of the Pr L_3-edge for a densified silica xerogel (10 000 ppm Pr/Si) and $4ZnO \cdot 3B_2O_3$ glasses (containing 0.5, 1, 2, 4 and 8 mol% of Pr) have been presented. The shape of the XANES signals confirms that the praseodymium in these materials is present as a Pr^{3+}.

The radial distribution functions for the first coordination shell of Pr^{3+} have been reconstructed from the EXAFS signals. The RDFs for all of the zinc borate glasses are similar and correspond to $\sim 6.9 \pm 0.7$ oxygen atoms with a broad distribution of Pr–O distances. The mean Pr–O distance $\langle R \rangle$ is about 2.53 Å and differs by ~ 0.06 Å from the position of the maximum $R_{MAX} = 2.47$ Å, due to an asymmetry of the distribution, appearing as a tail at longer distances. The shape of the distribution for the densified xerogel is more symmetric, with $\langle R \rangle = 2.46$ Å and $R_{MAX} = 2.47$ Å. The main difference between the densified xerogel and the glasses, in the first shell, is the average number of oxygen neighbours, which is $\sim 6.2 \pm 0.7$ in the xerogel; i.e. about 0.6 atom smaller than in the glasses.

EXAFS spectroscopy does not detect changes in the local environment of Pr^{3+} in the

$4ZnO \cdot 3B_2O_3$ glasses, as a function of the praseodymium content, nor in the next nearest neighbour shell, where there is evidence for the presence of contributions from Pr–B and Pr–Zn distances. No clustering is observed with increasing Pr content.

Acknowledgements

One of us (A.K.) wish to thank the Centro CNR-ITC di Fisica degli Stati Aggregati ed Impianto Ionico (Trento) for financial support and the Università di Trento for hospitality. The authors are grateful to Cristina Armellini, for excellent technical assistance in the sample preparation and to M. Ferrari and G. Pucker for useful discussions. The ESRF financially supported this project (HC511-1996). The authors are grateful to the staff of the GILDA beamline for assistance during the measurements.

References

[1] M.J. Weber, J. Non-Cryst. Solids 123 (1990) 208; E.J.A. Pope, in: Sol–Gel Optics II, SPIE Proc. 1758 (1992) 360.
[2] M. Ferrari, E. Duval, A. Boyrivent, A. Boukenter, J.L. Adam, J. Non-Cryst. Solids 99 (1988) 210.
[3] M. Bettinelli, A. Speghini, M. Montagna, M. Ferrari, J. Non-Cryst. Solids 201 (1996) 211; M. Sbetti, E. Moser, M. Montagna, M. Ferrari, S. Chaussedent, M. Bettinelli, J. Non-Cryst. Solids 220 (1997) 217.
[4] C. Armellini, L. Del Longo, M. Ferrari, M. Montagna, G. Puker, P. Sagoo, J. Sol–Gel Sci. Technol., in press; L. Del Longo, M. Ferrari, E. Zanghellini, M. Bettinelli, J.A. Capobianco, M. Montagna, F. Rossi, J. Non-Cryst. Solids, in press.
[5] A. Bouajai, M. Ferrari, M. Montagna, J. Sol–Gel Sci. Technol. 8 (1997) 391.
[6] B.C. Chakoumakos, M.M. Abraham, L.A. Boatner, Solid State Chem. 109 (1994) 197.
[7] A. Kuzmin, Physica B 208&209 (1995) 175; A. Kuzmin, J. Phys. IV (France) 7 (1997) C2–213.
[8] A. Kuzmin, J. Purans, G. Dalba, P. Fornasini, F. Rocca, J. Phys.: Condens. Matter 8 (1996) 9083; A. Kuzmin, J. Purans, SPIE Proc. 2968 (1997) 180.
[9] F. Rocca, A. Kuzmin, M. Ferrari, J. Non-Cryst. Solids, to be published.
[10] J.J. Rehr, J. Mustre de Leon, S.I. Zabinsky, R.C. Albers, J. Am. Chem. Soc. 113 (1991) 5135; J. Mustre de Leon, J.J. Rehr, S.I. Zabinsky, R.C. Albers, Phys. Rev. B 44 (1991) 4146.
[11] T.W. Capehart, R.K. Mishra, J.F. Herbst, J. Appl. Phys. 72 (1992) 676; J.M. Esteva, R.C. Karnatak, H. Dexpert, M. Gasgnier, P.E. Caro, L. Albert, J. Phys. IV (France) 47 (1986) C8-955; H. Arashi, S. Shin, H. Miura, A. Nakashima, M. Ishigame, O. Shimomura, Solid State Ionics 35 (1989) 323.
[12] G. Dalba, P. Fornasini, F. Rocca, Phys. Rev. B 47 (1993) 8502.
[13] C.W. Ponadar, G.E. Brown, Jr., Geochim. Cosmochim. Acta 53 (1989) 2893.
[14] A. Bouajaj, M. Ferrari, M. Montagna, E. Moser, A. Piazza, R. Campostrini, G. Carturan, Philos. Mag. B 71 (1995) 633.
[15] E.M. Larson, F.W. Lytle, P.G. Eller, R.B. Greegor, M.P. Eastman, J. Non-Cryst. Solids 116 (1990) 57.
[16] P.M. Peters, S.N. Houde-Walter, Appl. Phys. Lett. 70 (1997) 541.